Journal of Porous Media 7(4), 1–14 (2004)

Free Convection in a Shallow Annular Cavity Filled with a Porous Medium

D. M. Leppinen,[1]* I. Pop,[2] D. A. S. Rees,[3] and L. Storesletten[4]

[1]Centre for Mathematical Sciences, University of Cambridge, Wilberforce Road, Cambridge, CB3 0WA, UK;
*E-mail: D.M.Leppinen@damtp.cam.ac.uk
[2]Faculty of Mathematics, University of Cluj, R3400 Cluj, CP253, Romania
[3]Department of Mechanical Engineering, University of Bath, Claverton Down, Bath, BA2 7AY, UK
[4]Department of Mathematics, Agder University College, Serviceboks 422, 4604 Kristiansand, Norway

ABSTRACT

In this paper we use asymptotic analysis to examine free convection in a shallow annular cavity filled with a fluid-saturated porous medium. The sidewalls of the cavity are maintained at different temperatures and the upper and lower boundaries are insulating. Results are obtained in the limit as the aspect ratio A, defined as the ratio of the height of the annular cavity to its width, goes to zero. This problem was first studied by Pop, Rees, and Storesletten (J. Porous Media, vol. 1, pp. 227–241, 1998) who considered the case when $\delta = O(1/A)$ *where* δ *is the ratio of the inner cylinder radius to the height of the cavity. The results of Pop et al. are extended in this paper by considering convection in the limit as* $A \to 0$ *with* $\delta = O(1)$*. The results indicate that curvature effects strongly influence the nature of convection in shallow annular cavities.*

Received March 26, 2003; Accepted July 13, 2003

NOMENCLATURE

c_n^k, d_n^k, e_2^k, f_2^k	numerical constants in central core
C_n^k, D_n^k	numerical constants in hot end region
g	coefficient of gravity
h	height of annular gap
k	thermal conductivity
K	permeability
Nu	Nusselt number
r	dimensionless radial coordinate, $r = r^*/h$
$r_h(r_c)$	radius of inner (outer) cylinder
Ra	Rayleigh number, $\mathrm{Ra} = gK\beta\,(T_h - T_c)h/\alpha\nu$
T^*	dimensional temperature
$T_h(T_c)$	temperature of inner (outer) cylinder
u	dimensionless radial velocity
v	dimensionless vertical velocity
x	dimensionless displacement from inner cylinder, $x = r - \delta$
z	dimensionless vertical coordinate, $z = z^*/h$

Greek symbols

α	thermal diffusivity
β	thermal expansion coefficient
δ	dimensionless radius of inner cylinder, $\delta = r_1/h$
η	stretched asymptotic matching variable, $\eta = A^{\chi}r$
θ	dimensionless temperature, $\theta = (T^* - T_c)/(T_h - T_c)$
λ	logarithmic temperature profile parameter, $\lambda = 1/\ln\,(A\delta/(1 + A\delta))$
ν	kinematic viscosity
ξ	displacement from outer cylinder, $\xi = r - 1/A - \delta$
ρ	curvature parameter, $\rho = A\delta = r_h/(r_c - r_h)$
ϕ	perturbed temperature, $\phi = \theta - \theta_c$
χ	stretching factor used during asymptotic matching
ψ	cylindrical stream function

Superscripts

*	dimensional variable
$\sim$	hot end region variable
–	cold end region variable
$\wedge$	core region variable

INTRODUCTION

Pop, Rees, and Storesletten (1998) used asymptotic analysis to examine steady free convection in a shallow annular cavity between two concentric circular cylinders filled with a fluid-saturated porous medium. The top and bottom boundaries of the annular cavity were perfectly insulating and the inner cylinder was maintained at a higher temperature than the outer cylinder. Their results are valid in the limit as the aspect ratio A, defined as the ratio of the height of the cavity divided by its width, is small. Pop et al. (1998) have argued that this flow geometry is of relevance to the modeling of thermal energy storage tanks, petroleum reservoirs, chemical catalytic converters, and the insulation of gas-cooled reactor vessels.

In the limit of small Darcy number (i.e., when momentum transport can be modeled without including the Brinkman and Forchheimer terms in the Darcy equation), the heat transfer and fluid flow due to convection in cylindrical annuli depend on three parameters. First, the Rayleigh number Ra provides a measure of the strength of the thermal forcing to the diffusion of heat and momentum, with larger Ra leading to more vigorous convection. Second is a curvature parameter δ defined as the ratio of the

radius of the inner cylinder to the height of the annular gap. The term curvature is used to emphasize the fact that the heat transfer area in a cylindrical annulus increases in proportion to the radius when moving from the inner to the outer cylinder. Prasad and Kulacki (1984, 1985) and Prasad, Kulacki, and Kulkarni (1986) have already noted the importance of curvature to flows in annular cavities filled with porous media. Third is the aspect ratio A, which has been defined above. Pop et al. (1998) used asymptotic analysis to examine convection in the limit as $A \to 0$ with and Ra = $O(1)$ and Ra = $O(1/A)$. Their results were limited to the case of $\delta = O(1/A)$, where curvature effects are relatively unimportant.

Leppinen (2002), used asymptotic analysis to examine convection in a shallow cylindrical annulus filled with a Newtonian fluid (i.e., the nonporous medium analogue of the work by Pop et al., 1998). In both the porous and the nonporous medium cases, the flow can be divided into a central core region and two end-zone regions. The flow is approximately parallel in the central core, with fluid moving toward the cold cylinder in the top half of the cavity and fluid moving toward the hot cylinder in the bottom half of the cavity. The flow is turned around in end regions near the inner and outer cylinders, which are approximately square. Leppinen (2002) considered convection in the limit as $A \to 0$ with Ra = $O(1)$ for the case of $\delta = O(1/A)$ and $\delta = O(1)$. The purpose of this note is to extend the results of Pop et al. (1998) by examining convection in a porous medium when $\delta = O(1)$ with Ra = $O(1)$, where it is noted that the asymptotic analysis is fundamentally of the same form for flow in both a porous and nonporous medium. It is our belief that the flows described here are very likely to be observable in practice since the studies of Rees (1993) and Lewis et al. (1995) have demonstrated that vertical free convection from a uniform temperature plane heated surface is stable.

GOVERNING EQUATIONS

We consider convection in an annular cavity of height between an inner cylinder of radius $r^* = r_h$ that is maintained at temperature $T^* = T_h$ and an outer cylinder of radius $r^* = r_c$ that is maintained at a temperature of $T^* = T_c$ with (see Fig. 1). The enclosure is filled with a fluid-saturated porous medium that has kinematic viscosity ν, permeability K, and effective thermal diffusivity α. The top and bottom boundaries are insulating and all boundaries are rigid and impermeable. Following Pop et al. (1998), the governing equations are

$$\frac{\partial}{\partial r^*}(r^* u^*) + \frac{\partial}{\partial z^*}(r^* w^*) = 0 \tag{1}$$

$$\frac{\partial u^*}{\partial z^*} - \frac{\partial w^*}{\partial r^*} = -\frac{gK\beta}{\nu}\frac{\partial T^*}{\partial r^*} \tag{2}$$

$$u^*\frac{\partial T^*}{\partial r^*} + w^*\frac{\partial T^*}{\partial z^*} = \alpha\left(\frac{\partial^2 T^*}{\partial r^{*2}} + \frac{1}{r^*}\frac{\partial T^*}{\partial r^*} + \frac{\partial^2 T^*}{\partial z^{*2}}\right) \tag{3}$$

where u^* and w^* are the radial and axial Darcy velocities, respectively, g is the acceleration of gravity, and β is the thermal expansion coefficient. In writing Eqs. (1)–(3) it has been assumed that the flow is axisymmetric about the z^* axis, steady, and that it obeys Darcy's Law and the Boussinesq approximation.

We introduce the stream function ψ^* defined by

$$u^* = -\frac{1}{r^*}\frac{\partial \psi^*}{\partial z^*} \quad \text{and} \quad w^* = \frac{1}{r^*}\frac{\partial \psi^*}{\partial r^*} \tag{4}$$

and nondimensionalize the governing equations using

$$r = r^*/h\,, \quad z = z^*/h\,,$$

$$\psi = \psi^*/(h\alpha\,\mathrm{Ra})\,, \quad \text{and} \quad \theta = (T^* - T_c)/(T_h - T_c) \tag{5}$$

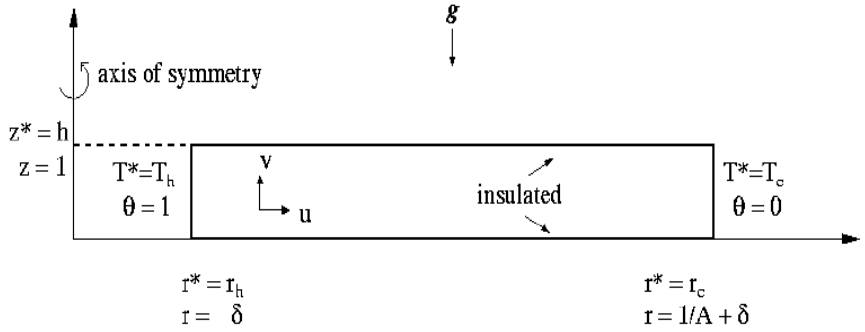

Figure 1. Schematic of annular enclosure.

where

$$\mathrm{Ra} = \frac{gK\beta(T_h - T_c)h}{\alpha\nu} \tag{6}$$

is the Rayleigh number to give

$$\frac{1}{r}\left(\frac{\partial^2\psi}{\partial r^2} + \frac{\partial^2\psi}{\partial z^2}\right) - \frac{1}{r^2}\frac{\partial\psi}{\partial r} = \frac{\partial\theta}{\partial r} \tag{7}$$

$$\frac{\partial^2\theta}{\partial r^2} + \frac{1}{r}\frac{\partial\theta}{\partial r} + \frac{\partial^2\theta}{\partial z^2} = \frac{\mathrm{Ra}}{r}\left(\frac{\partial\psi}{\partial r}\frac{\partial\theta}{\partial z} - \frac{\partial\psi}{\partial z}\frac{\partial\theta}{\partial r}\right) \tag{8}$$

The aspect ratio of the cavity is $A = h/(r_c - r_h)$ and the curvature parameter is $\delta = r_h/h$. The governing equations must be solved subject to $\psi = \dfrac{\partial\theta}{\partial z} = 0$ when $z = 0,1$, $\psi = 0$, $\theta = 1$ when $r = \delta$, and $\psi = \theta = 0$ when $r = \delta + 1/A$. The solution procedure will be to obtain asymptotic expansions in the central core region and to match these solutions to asymptotic expansions near the hot and cold end regions.

ASYMPTOTIC ANALYSIS WHEN $\delta = O(1/A)$

The asymptotic analysis and solution procedure when $\delta = O(1/A)$ is given in Pop et al. (1998) and only the results that are necessary to understand the solution procedure when $\delta = O(1)$ are repeated here. The key feature of the analysis when $\delta = O(1/A)$ is that $r = O(1/A)$ throughout the entire domain and the effects of curvature are comparable in each of the hot end, the central core, and the cold end regions. The analysis begins by introducing the variable $x = r - \delta$ into Eqs. (7) and (8) so that $1/r\,(A\delta + Ax) = A/(\rho + Ax)$ where $\rho = A\delta = O(1)$ as $A \to 0$. This substitution explicitly introduces a small parameter into Eqs. (7) and (8) and asymptotic solutions of the form

$$(\psi, \theta) = \sum_{i=0}^{N} A^i(\psi_i, \theta_i) \tag{9}$$

can be determined. In particular, in the central core the temperature profile is

$$\theta = \lambda \ln\left(\frac{\rho + Ax}{\rho + 1}\right) + A^2\left[\frac{-\lambda^2\mathrm{Ra}}{(\rho + Ax)^2}\left(\frac{z^3}{6} - \frac{z^2}{4} + \frac{1}{24}\right) + \frac{\mathrm{Ra}^2\lambda^3}{240(\rho + Ax)sp2} - \frac{\mathrm{Ra}^2\lambda^4}{240}\times\left(\frac{2\rho + 1}{\rho^2\,(\rho + 1)^2}\ln\,(\rho + Ax) + \frac{\ln(\rho)}{\rho + 1)^2} - \frac{\ln(\rho + 1)}{\rho^2}\right)\right] + O(A^3) \tag{10}$$

where

$$\lambda = \frac{1}{\ln\left(\dfrac{A\delta}{A\delta + 1}\right)} \tag{11}$$

(see Pop et al., 1998, for details and the corresponding result for ψ). This core region solution is fully specified by examining the governing equations in the core region and then matching with solutions in the hot and cold end regions. As noted by Pop et al. (1998), the governing equations in the core region are such that the solution at $O(A^n)$ can only be determined by examining the governing equations at $O(A^{n+2})$. As will be shown below, this feature carries over to the analysis for the case when $\delta = O(1)$.

ASYMPTOTIC ANALYSIS WHEN $\delta = O(1)$

The asymptotic analysis when $\delta = O(1)$ is complicated by the fact that curvature effects are relatively important in the hot end region and relatively unimportant in the central core and cold end region. In the hot end $1/r = O(1)$ while in the central core and the cold end region $1/r = O(A)$. Thus, in the central core and the cold end region a perturbation parameter can be introduced into the governing equations by rescaling the radial coordinate. As it stands, however, the governing equations in the hot end region are Eqs. (7) and (8). Unfortunately, each of the terms in these equations is of the same order of magnitude and there is no small parameter available to perturb. If we were to use an expansion of the form of Eq. (9) for the case of $\delta = O(1)$, we would have to solve the full nonlinear, coupled stream function and energy equations at each order in A in the hot end region. To avoid this complication, we make a substitution of the form

$$\theta = \phi + \theta_c \tag{12}$$

where

$$\theta_c = \lambda \ln\left(\frac{Ar}{1 + A\delta}\right) \tag{13}$$

is the conduction temperature profile between cylinders of radius $r = \delta$ and $r = \delta + 1/4$. This substitution is motivated

by observing that the leading order temperature profile for the case of $\delta = O(1/A)$ is precisely the conduction profile [cf. Eq. (11)]. Upon substitution of Eq. (12), Eqs. (7) and (8) become

$$\frac{1}{r}\left(\frac{\partial^2\psi}{\partial r^2}+\frac{\partial^2\psi}{\partial z^2}\right)-\frac{1}{r^2}\frac{\partial\psi}{\partial r}=\frac{\partial\phi}{\partial r}+\frac{\lambda}{r} \tag{14}$$

$$\frac{\partial^2\phi}{\partial r^2}+\frac{1}{r}\frac{\partial\phi}{\partial r}+\frac{\partial^2\phi}{\partial z^2} = \frac{\mathrm{Ra}}{r}\left(\frac{\partial\psi}{\partial r}\frac{\partial\phi}{\partial z}-\frac{\partial\psi}{\partial z}\frac{\partial\phi}{\partial r}\right)-\frac{\mathrm{Ra}\lambda}{r^2}\frac{\partial\psi}{\partial z} \tag{15}$$

This substitution has introduced the perturbation parameter λ into the governing equations, where it is noted that λ is asymptotically small as $A \to 0$. By examining Eqs. (14) and (15) and by noting that $1/r = O(A)$ throughout the central core and cold end region, we seek asymptotic expansions of the form

$$(\psi,\phi)=\sum_{i=0}^{N}A^i\sum_{k=0}^{\infty}\lambda^k(\psi_i^k,\phi_i^k) \tag{16}$$

where it is noted that, in order to obtain an asymptotic solution, the inner summation must be performed before the outer summation.

Solution Methodology

Our objective is to determine the first convective influence (i.e., Rayleigh number dependence) to the temperature and stream function fields in the central core. This will be accomplished by matching asymptotic solutions in the central core region with asymptotic solutions in the hot and cold end regions. It will be shown that matching between the hot end region and the central core is complicated by the fact that terms for the central core solution jump order when matching [i.e., terms that appear to be $O(A^2)$ are actually $O(1)$]. The first convective influence in the central core will occur at $O(\lambda^4)$, although a complete analysis to higher orders in A is required to show this. Due to the need to solve the governing equations in the hot end region numerically, matching is not performed beyond this order.

Central Core

In the central core we note that $r = O(1/A)$, so we rescale the radial coordinate using $\hat{r} = Ar$. Denoting the stream function and temperature perturbation in the central core by $\hat{\psi}$ and $\hat{\phi}$, the core equations become

$$\frac{1}{\hat{r}}\frac{\partial^2\hat{\psi}}{\partial z^2}+A^2\left(\frac{\partial^2\hat{\psi}}{\partial\hat{r}^2}-\frac{1}{\hat{r}^2}\frac{\partial\hat{\psi}}{\partial\hat{r}}\right)=\frac{\partial\hat{\phi}}{\partial\hat{r}}+\frac{\lambda}{\hat{r}} \tag{17}$$

$$\frac{\partial^2\hat{\phi}}{\partial z^2}+A^2\left(\frac{\partial^2\hat{\phi}}{\partial\hat{r}^2}+\frac{1}{\hat{r}}\frac{\partial\hat{\phi}}{\partial\hat{r}}\right) = A^2\frac{\mathrm{Ra}}{\hat{r}}\left(\frac{\partial\hat{\psi}}{\partial\hat{r}}\frac{\partial\hat{\phi}}{\partial z}-\frac{\partial\hat{\psi}}{\partial z}\frac{\partial\hat{\phi}}{\partial\hat{r}}\right)-A^2\frac{\mathrm{Ra}\lambda}{\hat{r}^2}\frac{\partial\hat{\psi}}{\partial z} \tag{18}$$

These equations must be solved using expansions of the form of Eq. (16), where it is noted that the only boundary conditions available in the central core are $\hat{\psi}=\frac{\partial\hat{\phi}}{\partial z}=0$ when $z = 0,1$.

The energy equation at $O(\lambda^k)$ is

$$\frac{\partial^2\hat{\phi}_0^k}{\partial z^2}=0 \tag{19}$$

Integrating this equation and applying the boundary condition $\frac{\partial\hat{\phi}_0^k}{\partial z}=0$ when $z=0,1$ gives

$$\frac{\partial\hat{\phi}_0^k}{\partial z}\equiv 0 \tag{20}$$

and hence $\hat{\phi}_0^k = g_0^k(\hat{r})$ where g_0^k is a function of $\hat{r}$ only, which has yet to be determined. The value of $\hat{\phi}_0^k$ cannot be determined by examining the governing equations at $O(\lambda^k)$. Instead, as will be shown below, $\hat{\phi}_0^k$ is only fully specified by proceeding to $O(A^2\lambda^k)$. For simplicity, Eq. (20) will be written in the equivalent form

$$\frac{\partial\hat{\phi}_0^k}{\partial\hat{r}}=\frac{c_0^k}{\hat{r}} \tag{21}$$

where c_0^k is a yet to be determined function of $\hat{r}$.

The stream function equation at $O(\lambda^k)$ is

$$\frac{1}{\hat{r}}\frac{\partial^2\hat{\psi}_0^k}{\partial z^2}=\frac{\partial\hat{\phi}_0^k}{\partial\hat{r}}+\delta_{k,1}\frac{1}{\hat{r}} \tag{22}$$

where $\delta_{m,n} = 1$ if $m = n$ and is equal to 0 otherwise. Upon substitution of Eq. (21) into Eq. (22), we obtain

$$\frac{\partial^2\hat{\psi}_0^k}{\partial z^2}=c_0^k+\delta_{k,1} \tag{23}$$

Integrating this equation twice with respect to z and applying the boundary conditions gives

$$\hat{\psi}_0^k = \frac{1}{2}(c_0^k + \delta_{k,1})(z^2 - z) \tag{24}$$

The governing equations at $O(A\lambda^k)$ are

$$\frac{\partial^2 \hat{\phi}_1^k}{\partial z^2} = 0 \quad \text{and} \quad \frac{1}{\hat{r}}\frac{\partial^2 \hat{\psi}_1^k}{\partial z^2} = \frac{\partial \hat{\phi}_1^k}{\partial \hat{r}} \tag{25}$$

and using the same solution procedure as above, we obtain

$$\frac{\partial \hat{\phi}_1^k}{\partial \hat{r}} = \frac{c_1^k}{\hat{r}} \quad \text{and} \quad \hat{\psi}_1^k = \frac{1}{2}c_0^k(z^2 - z) \tag{26}$$

where c_1^k is a yet to be determined function of $\hat{r}$.

The energy equation at $O(A^2\lambda^k)$ is

$$\frac{\partial^2 \hat{\phi}_2^k}{\partial z^2} + \frac{\partial^2 \hat{\phi}_0^k}{\partial \hat{r}^2} + \frac{1}{\hat{r}}\frac{\partial \hat{\phi}_0^k}{\partial \hat{r}} = \sum_{m+n=k} \frac{\mathrm{Ra}}{\hat{r}}\left(\frac{\partial \hat{\psi}_0^m}{\partial \hat{r}}\frac{\partial \hat{\phi}_0^n}{\partial z} - \frac{\partial \hat{\psi}_0^m}{\partial z}\frac{\partial \hat{\phi}_0^n}{\partial \hat{r}}\right) - \frac{\mathrm{Ra}\lambda}{\hat{r}^2}\frac{\partial \hat{\psi}_0^{k-1}}{\partial z} \tag{27}$$

which upon substitution of Eqs. (21) and (24) becomes

$$\frac{\partial^2 \hat{\phi}_2^k}{\partial z^2} + \frac{1}{\hat{r}}\frac{\partial c_0^k}{\partial \hat{r}} = -e_2^k \frac{\mathrm{Ra}}{\hat{r}^2}(2z - 1) \tag{28}$$

where

$$e_2^k = \frac{1}{2}(c_0^{k-1} + \delta_{1,k-1}) + \sum_{m+n=k} \frac{1}{2}c_0^n(c_0^m + \delta_{1,m}) \tag{29}$$

In the definition of e_2^k and in all other cases where there is a summation over ordered pairs (m, n) with $m + n = k$, both m and n must be greater than 0. Integrating Eq. (28) from $z = 0$ to 1 and applying the boundary conditions that

$\frac{\partial \hat{\phi}_2^k}{\partial z} = 0$ when $z = 0,1$ gives

$$\frac{\partial c_0^k}{\partial \hat{r}} = 0 \tag{30}$$

so that c_0^k is a numerical constant. Thus Eq. (21) can be integrated to give

$$\hat{\phi}_0^k = c_0 spk \ln \hat{r} + d_0^k \tag{31}$$

where the unknown constants c_0^k, d_0^k will be determined by matching with the hot and cold end regions.

It is noted that the solution at $O(\lambda^k)$ has only now been determined by proceeding to $O(A^2\lambda^k)$ in the perturbation analysis. It is a general feature of Eqs. (17) and (18) that the complete solution at $O(A^n\lambda^k)$ can only be determined by proceeding to $O(A^{n+2}\lambda^k)$ in the perturbation analysis. This is because there are not enough boundary conditions available in the core region to fully solve the partial differential equations for $\hat{\psi}_n^k$ and $\hat{\phi}_n^k$.

The energy equation at $O(A^2\lambda^k)$ is solved by integrating Eq. (28) twice with respect to z and applying the appropriate boundary conditions to give

$$\hat{\phi}_2^k = -\frac{\mathrm{Ra}}{\hat{r}^2}e_2^k\left(\frac{1}{3}z^3 - \frac{1}{2}z^2 + \frac{1}{12}\right) + \tau_2^k \tag{32}$$

where τ_2^k is a yet to be determined function of $\hat{r}$. The $\frac{1}{12}$ in Eq. (32) has been included so that the polynomial is symmetric about $z = 1/2$. This is acceptable since τ_2^k is an arbitrary function of $\hat{r}$.

The stream function equation at $O(A^2\lambda^k)$ simplifies to

$$\frac{\partial^2 \hat{\psi}_2^k}{\partial z^2} = \hat{r}\frac{\partial \hat{\phi}_2^k}{\partial \hat{r}} \tag{33}$$

which can be integrated to give

$$\hat{\psi}_2^k = e_2^k \times \frac{2\mathrm{Ra}}{\hat{r}^2}\left(\frac{1}{60}z^5 - \frac{1}{24}z^4 + \frac{1}{24}z^2 - \frac{1}{60}z\right) + \frac{\hat{r}}{2}\frac{d\tau_2^k}{d\hat{r}}\left(z^2 - z\right) \tag{34}$$

The governing equations at $O(A^3\lambda^k)$ can be solved in a similar manner to those at $O(A^2\lambda^k)$. For our current purposes, it is sufficient to note that the energy equation at $O(A^3\lambda^k)$ can be used to completely specify the solution at $O(A\lambda^k)$. In particular, it can be shown that c_1^k is a numerical constant and Eq. (26) can be solved to give

$$\phi_1^k = c_1^k \ln(\hat{r}) + d_1^k \tag{35}$$

where the numerical constants c_1^k and d_1^k must be determined by matching with the end regions.

The energy equation at $O(A^4\lambda^k)$ is

$$\frac{\partial^2 \hat{\phi}_4^k}{\partial z^2} + \frac{\partial^2 \hat{\phi}_2^k}{\partial \hat{r}^2} + \frac{1}{\hat{r}}\frac{\partial \hat{\phi}_2^k}{\partial \hat{r}} = \sum_{m+n=k} \frac{\mathrm{Ra}}{\hat{r}}\left(\frac{\partial \hat{\psi}_0^m}{\partial \hat{r}}\frac{\partial \hat{\phi}_2^n}{\partial z} - \frac{\partial \hat{\psi}_0^m}{\partial z}\frac{\partial \hat{\phi}_2^n}{\partial \hat{r}} + \times\frac{\partial \hat{\psi}_1^m}{\partial \hat{r}}\frac{\partial \hat{\phi}_1^n}{\partial z} - \frac{\partial \hat{\psi}_1^m}{\partial z}\frac{\partial \hat{\phi}_1^n}{\partial \hat{r}} + \frac{\partial \hat{\psi}_2^m}{\partial \hat{r}}\frac{\partial \hat{\phi}_0^n}{\partial z} - \frac{\partial \hat{\psi}_2^m}{\partial z}\frac{\partial \hat{\phi}_0^n}{\partial \hat{r}}\right) -$$

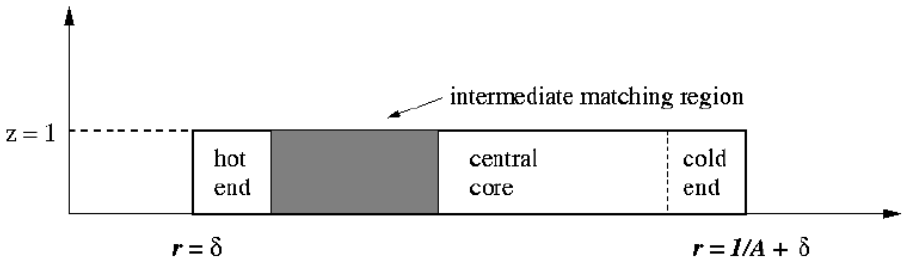

Figure 2. Intermediate matching region when $A \to 0$ with δ of $O(1)$.

$$\times \frac{\mathrm{Ra}}{\hat{r}^2}\frac{\partial \hat{\psi}_2^{k-1}}{\partial z} \tag{36}$$

and the objective is to use this equation to fully specify $\hat{\phi}_2^k$. This is achieved by first substituting known values into Eq. (36) and then integrating from $z = 0$ to $z = 1$ and using the appropriate boundary conditions to give

$$\frac{\partial^2 \tau_2^k}{\partial \hat{r}^2} + \frac{1}{\hat{r}}\frac{\partial \tau_2^k}{\partial \hat{r}} = \frac{-2\mathrm{Ra}^2}{\hat{r}^4}\int_0^1 f_2^k \left(\frac{1}{3}z^3 - \frac{1}{2}z^2 + \frac{1}{12}\right)\left(z - \frac{1}{2}\right)dz \tag{37}$$

where

$$f_2^k = \sum_{m+n=k} e_2^n (c_0^m + \delta_{1,m}) \tag{38}$$

Equation (37) can be integrated to give

$$\tau_2^k = c_2^k \ln(\hat{r}) + d_2^k + f_2^k \frac{\mathrm{Ra}^2}{120}\frac{1}{\hat{r}^2} \tag{39}$$

where the numerical constants c_2^k and d_2^k must be determined by matching with solutions in the end regions. Substitution of Eq. (39) into (34) will fully specify the value of $\hat{\psi}_2^k$.

An examination of Eqs. (32), (34), and (39) reveals that some of the terms in the asymptotic expansion in the core region jump order when matching with solutions in the hot end region. To accommodate this, the matching is performed using an intermediate variable $\eta = rA^\chi = \hat{r}A^{\chi-1}$, where $0 < \chi < 1$. (For a detailed discussion of intermediate matching, see the book by Hinch, 1991.) Matching is performed by expressing the core region solutions and the hot end region solutions in terms of η and then ensuring that the solutions have the identical form throughout the entire intermediate matching region (see Fig. 2). For a fixed value of , the intermediate matching region becomes infinite as $A \to 0$. Observing that

$$\frac{A^2}{\hat{r}^2} = \frac{1}{\eta^2}A^{2\chi} = \frac{1}{r^2} \tag{40}$$

it follows that the $1/\hat{r}^2$ terms that occur at $O(A^2)$ in the core region must be matched with $1/r^2$ terms at $O(1)$ in the hot end region. To complicate matters further, it can be shown that for all $n \geq 1$ there are terms in the core region solutions at $O(A^{2n})$ that vary as $1/\hat{r}^{2n}$ and hence jump to $O(1)$ when matching with solutions in the hot end region. For the purposes of this paper, matching can be performed by determining the terms in the solutions for $\hat{\phi}_{2n}^2$, $\hat{\psi}_{2n}^2$, and $\hat{\phi}_{2n}^3$ that jump order when matching with the hot end region solutions. Recursion relations for these higher order solutions can easily be derived and solved using the known starting values of $\hat{\phi}_2^2$, $\hat{\psi}_2^2$, and $\hat{\phi}_2^3$.

Cold End Region

The governing equations in the cold end region are obtained from Eqs. (14) and (15) by introducing $\xi = \delta + 1/A - r$ as the radial variable where ξ measures the radial distance from the cold cylinder. If overbars are used to denote the cold end region solutions, then the matching condition for the temperature field between the core and cold end region is given by

$$\lim_{\hat{r}\to 1+A\delta} \phi_n^k \sim \lim_{\xi\to\infty} \bar{\phi}_n^k$$

where it is noted that, when matching with the cold end region, no terms in the core region solution jump order. For the current purposes, matching will only be performed for $n = 0$.

At $O(\lambda^k)$, the governing equation in the cold end region are

$$\frac{\partial^2 \bar{\phi}_0^k}{\partial \xi^2} + \frac{\partial^2 \bar{\phi}_0^k}{\partial z^2} = 0 \quad \text{and} \quad \frac{\partial \bar{\phi}_0^k}{\partial \xi} = 0 \tag{41}$$

Combining the above equations with the boundary conditions $\frac{\partial \bar{\phi}_0^k}{\partial z} = 0$ when $z = 0,1$ and $\bar{\phi}_0^k = 0$ when $\xi = 0$ requires $\bar{\phi}_0^k = 0$ for all k. The solution to the energy equation at $O(\lambda^k)$ in the core region is simply $\hat{\phi}_0^k = c_0^k \ln \hat{r} + d_0^k$. By expressing $\hat{\phi}_0^k$ in terms of ξ, the matching condition is given by $c_0^k \ln (1 + A(\delta - \xi)) + d_0^k \sim \bar{\phi}_0^k = 0$ which can be expanded to give

$$c_0^k (A(\delta - \xi) - 1/2 A^2 (\delta - \xi)^2 + \ldots) + d_0^k \sim 0 \tag{42}$$

Hence to leading order in A, $d_0^k = 0$ for all k.

Hot End Region

The solutions in the hot end region will be denoted as $\psi = \tilde{\psi}$ and $\phi = \tilde{\phi}$, where it is noted that the governing equations in the hot end region are given be Eqs. (14) and (15) without any rescaling. Matching between the hot end region and the core region is complicated by the fact that terms jump order when attempting to match. The matching proceeds by first examining the general form of $\tilde{\phi}_0^k$ throughout the intermediate matching region and noting that the matching procedure involves two steps–the first is performed analytically and the second is performed numerically.

The energy equation in the hot end region at $O(\lambda^k)$ can be written as

$$\frac{\partial^2 \tilde{\phi}_0^k}{\partial r^2} + \frac{1}{r}\frac{\partial \tilde{\phi}_0^k}{\partial r} + \frac{\partial^2 \tilde{\phi}_0^k}{\partial z^2} = f(r, z) \tag{43}$$

where $f(r, z)$ is a forcing function that can be written explicitly by examining Eq. (15). The general solution to Eq. (43) is $\tilde{\phi}_0^k = (\tilde{\phi}_0^k)_h + (\tilde{\phi}_0^k)_{nh}$ where $(\tilde{\phi}_0^k)_h$ is the homogeneous solution to Eq. (43) with $f(r, z)$ replaced by 0, and $(\tilde{\phi}_0^k)_{nh}$ is a particular solution to nonhomogeneous Eq. (43) when $f(r, z) \neq 0$. The boundary conditions on $\tilde{\phi}_0^k$ are $\tilde{\phi}_0^k = 0$ when $r = \delta$, and $\frac{\partial \tilde{\phi}_0^k}{\partial z} = 0$ when $z = 0,1$. Moreover, $(\tilde{\phi}_0^k)_h$ and $(\tilde{\phi}_0^k)_{nh}$ must be of the correct form to match with solutions from the core region. Noting that the core region solutions behave as the sum of logarithmic terms, constant terms and terms that jump order with a radial dependence of $1/r^{2n}$ in the intermediate matching region, it follows that the hot end region solutions must display the same behavior in the intermediate matching region. The homogeneous solution to Eq. (43) that satisfies all of the boundary conditions and that is of the correct form to match with the core region solutions is simply $\tilde{\phi}_0^k = C_0^k \ln (r/\delta)$, where C_0^k is a numerical constant that must be determined by matching. Thus, to ensure that the hot end regions solutions are of the correct form to match with the core region solutions, it follows that the particular nonhomogeneous solution to Eq. (43) must behave as

$$(\tilde{\phi}_0^k)_{nh} \sim D_0^k + J_0^k(r, z) \tag{44}$$

throughout the intermediate matching region, where D_0^k is an as of yet undetermined numerical constant and where $J_0^k(r, z)$ is used to denote the sum of terms that jump to order $O(\lambda^k)$ when matching between the core region and the hot end region.

Logarithmic and Constant Terms

The first step in matching involves matching the logarithmic and constant terms in the core region with the corresponding terms in the hot end region, and the matching is performed using the intermediate variable $\eta = rA^\chi = \hat{r}A^{\chi-1}$ where $0 < \chi < 1$. The matching condition is

$$\sum_{k=1}^{\infty} \lambda^k (C_0^k \ln(r/\delta) + D_0^k) \sim \sum_{k=1}^{\infty} \lambda^k (c_0^k \ln \hat{r} + d_0^k) \tag{45}$$

which is expanded to yield

$$C_0^1 \chi \lambda \ln(1/A) + (C_0^1 \ln(\eta/\delta) + D_0^1)\lambda + C_0^2 \chi \lambda^2 \ln(1/A) + \ldots \sim$$
$$c_0^1(\chi - 1)\lambda \ln(1/A)$$
$$+ (c_0^1 \ln \eta + d_0^1)\lambda + c_0^2(\chi - 1)\lambda^2 \ln(1/A) + \ldots \tag{46}$$

By expanding Eq. (11) in terms of A as $A \to 0$, it can be shown that

$$\lambda \ln(1/A)$$
$$= -1 + \lambda(\ln \delta - (A\delta) + \frac{1}{2}(A\delta)^2 - \frac{1}{3}(A\delta)^3 - \ldots) \tag{47}$$

Thus, to leading order in A, $\lambda \ln (1/A) = -1 + \lambda \ln \delta$, and when this substitution is made into Eq. (46) and the coeffi-

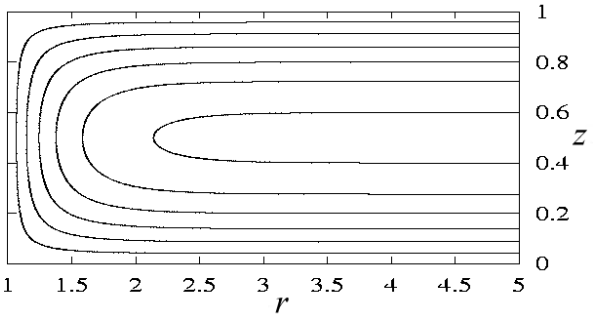

Figure 3. Leading order stream function $\tilde{\psi}_0^1$ in the hot end region when $\delta = 1$. The contours are $\tilde{\psi}_0^1$ = –0.02, –0.04, ..., –0.12 from the outside inwards.

cients of the powers of λ are compared, it is seen that $C_0^1\chi = c_0 sp1\ (\chi - 1)$ and

$$C_0^k \ln(\eta/\delta) + D_0^k + C_0^k \chi \ln\delta - C_0^{k+1}\chi = c_0^k \ln\eta + d_0^k + c_0^k(\chi - 1)\ln\delta - c_0^{k+1}(\chi - 1) \tag{48}$$

for $k > 1$. Since Eq. (48) must be satisfied for all values of $0 < \chi < 1$, it follows that $C_0^1 = c_0^1 = 0$, and that $C_0^k = c_0^k$ with $D_0^k = d_0^k + c_0^{k+1}$ when $k > 1$. Matching in the cold end region has shown that $d_0^k = 0$ for all k, so it follows that $c_0^{k+1} = C_0^{k+1} = D_0^k$.

Nonhomogeneous Solutions

While the above analysis has shown how the constants D_0^k are matched with solutions in the core region, the numerical value of these constants can only be determined by calculating the nonhomogeneous solutions noted in Eq. (44). The energy equation at $O(\lambda)$ in the hot end region is

$$\frac{\partial^2\tilde{\phi}_0^1}{\partial r^2} + \frac{1}{r}\frac{\partial\tilde{\phi}_0^1}{\partial r} + \frac{\partial^2\tilde{\phi}_0^1}{\partial z^2} = 0 \tag{49}$$

and the only solution that satisfies the appropriate boundary conditions and that can be matched with the core region solutions is $\tilde{\phi}_0^1 = C_0^1 \ln(r/\delta)$. (At $O(\lambda)$ there are no terms in the core region solutions that jump order.) Noting from above that $C_0^1 = 0$, it follows that $\tilde{\phi}_0^1 = 0$. Since Eq. (49) is homogenous, it follows that there is no nonhomogeneous solution and that $D_0^1 = 0$. This, in turn, implies that $C_0^2 = c_0^2 = 0$ so that the homogeneous solution at $O(\lambda^2)$ vanishes.

The stream function equation at $O(\lambda)$ is

$$\frac{1}{r}\left(\frac{\partial^2\tilde{\psi}_0^1}{\partial r^2} + \frac{\partial^2\tilde{\psi}_0^1}{\partial z^2}\right) - \frac{1}{r^2}\frac{\partial\tilde{\psi}_0^1}{\partial r} = \frac{1}{r}. \tag{50}$$

The boundary conditions on $\tilde{\psi}_0^1$ are $\tilde{\psi}_0^1 = 0$ when z = 0 and when $r = \delta$. Throughout the entire matching region, $\tilde{\psi}_0^1$ must satisfy $\tilde{\psi}_0^1 \sim \frac{1}{2}(z^3 - z)$. The solution of Eq. (50) is plotted in Fig. 3 for the specific value of $\delta = 1$. (The solution for other values of δ has the same general features as for $\delta = 1$). It is seen that the leading order stream function smoothly turns the flow through 180°. Equation (50) was solved using a standard second-order central differencing technique. The radial coordinate was truncated at $r = \delta + 16$ (although data is only plotted between $r = \delta$ and $r = \delta + 4$ in Fig. 3) and numerical solutions were obtained on a uniform 2048 by 128 (radial by vertical) grid. (Preliminary calculations were performed on much coarser grids and it is felt that the results presented herein are effectively grid independent.)

The energy equation at $O(\lambda^2)$ simplifies to

$$\frac{\partial^2\tilde{\phi}_0^2}{\partial r^2} + \frac{1}{r}\frac{\partial\tilde{\phi}_0^2}{\partial r} + \frac{\partial^2\tilde{\phi}_0^2}{\partial z^2} = -\frac{\mathrm{Ra}}{r^2}\frac{\partial\tilde{\psi}_0^1}{\partial z} \tag{51}$$

subject to $\tilde{\phi}_0^2 = 0$ when $r = \delta$, and $\frac{\partial\tilde{\phi}_0^2}{\partial z} = 0$ when $z = 0,1$. The matching condition for $\tilde{\phi}_0^2$ is

$$\tilde{\phi}_0^2 \sim C_0^2 \ln(r/\delta) + D_0^2 + (A^2\hat{\phi}_2^2 + A^4\hat{\phi}_4^2 + A^6\hat{\phi}_6^2 + \ldots) \tag{52}$$

throughout the intermediate matching region, where it is noted that the homogeneous part of the solution $(\tilde{\phi}_0^2)_h = C_0^2 \ln(r/\delta)$ can in fact be neglected since $C_0^2 = 0$.

The value of the constant D_0^2 can be determined by integrating Eq. (51) from $z = 0,1$ to give

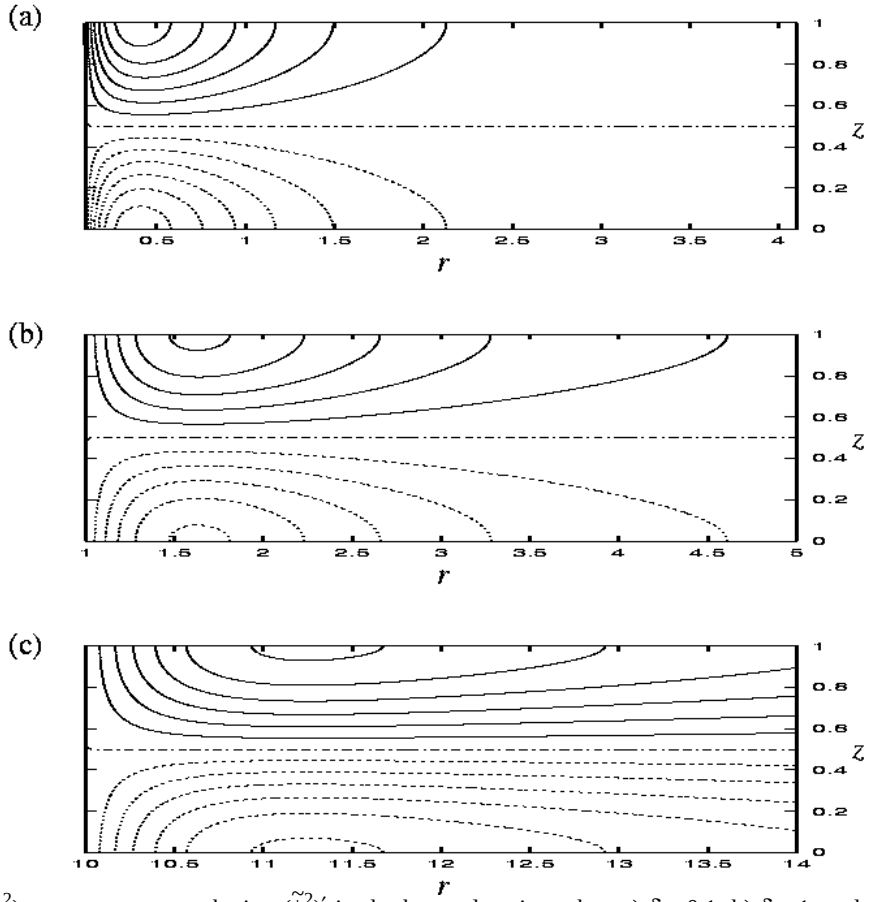

Figure 4. The $O(\lambda^2)$ temperature perturbation $(\tilde{\phi}_0^2)'$ in the hot end region when a) $\delta = 0.1$, b) $\delta = 1$, and c) $\delta = 10$. (See Table 1 for details.)

$$\int_0^1 \left(\frac{\partial^2 \tilde{\phi}_0^2}{\partial r^2} + \frac{1}{r}\frac{\partial \tilde{\phi}_0^2}{\partial r} + \frac{\partial^2 \tilde{\phi}_0^2}{\partial z^2} \right) dz = 0 \tag{53}$$

This equation is valid in the hot end region and throughout the entire intermediate matching region. Since $\tilde{\phi}_0^2 = 0$ when $\delta = 0$, Eq. (53) can be integrated twice with respect to r to give

$$\int_0^1 \tilde{\phi}_0^2 dz = (C_0^2)' \ln(r/\delta) \tag{54}$$

where $(C_0^2)'$ is a numerical constant of integration. Since it can be shown that $\int_0^1 \hat{\phi}_{2n}^2 dz = 0$ for all n, substitution of the matching condition of Eq. (52) into Eq. (53) yields $(C_0^2)' = C_0^2$ and more importantly $D_0^2 = 0$. This implies that $C_0^3 = c_0^3 = 0$.

Equation (51) can be rewritten using $\tilde{\phi}_0^2 = \mathrm{Ra}\,(\tilde{\phi}_0^2)'$ to give

$$\frac{\partial^2 (\tilde{\phi}_0^2)'}{\partial r^2} + \frac{1}{r}\frac{\partial (\tilde{\phi}_0^2)'}{\partial r} + \frac{\partial^2 (\tilde{\phi}_0^2)'}{\partial z^2} = -\frac{1}{r^2}\frac{\partial \tilde{\psi}_0^1}{\partial z} \tag{55}$$

The matching condition for $(\tilde{\phi}_0^2)'$ is obtained from Eq. (52) by setting $C_0^2 = D_0^2 = 0$. Equation (55) was solved using a second-order central difference formulation using the same numerical grids that were employed to calculate $\tilde{\psi}_0^1$. During the numerical integration, the sum given in Eq. (52) was truncated at $O(A^{10})$. The numerically determined solution of Eq. (55) is plotted in Fig. 4 for $\delta = 0.1$, 1 and 10. The minimum, maximum, and contour increment values for Fig. 4 are listed in Table 1. In all cases, the $O(\lambda^2)$ correction to the temperature field leads to positive perturbations in the top half of the enclosure, and negative perturbations in the bottom half of the enclosure. The perturbations are considerably larger for smaller values of δ, and the contours become more tightly bunched near the

Table 1

The minimum, maximum, and contour increments for the plots in Figs. 4 and 5. Positive (negative) contours are printed as solid (dashed) lines, and zero is plotted as a dot-dashed line

Figure	Minimum	Maximum	Increment
4(a)	-6×10^{-2}	6×10^{-2}	1×10^{-2}
4(b)	-1×10^{-2}	1×10^{-2}	2×10^{-3}
4(c)	-3×10^{-4}	3×10^{-4}	5×10^{-5}
5(a)	-8×10^{-4}	8×10^{-4}	1×10^{-4}
5(b)	-3×10^{-4}	3×10^{-4}	1×10^{-4}
5(c)	-7×10^{-5}	7×10^{-5}	1×10^{-5}

inner cylinder for smaller values of δ, indicating the increased influence of curvature for smaller values of δ. The stream function equation at $O(\lambda^2)$ is

$$\frac{1}{r}\left(\frac{\partial^2\tilde{\psi}_0^2}{\partial r^2}+\frac{\partial^2\tilde{\psi}_0^2}{\partial z^2}\right)-\frac{1}{r^2}\frac{\partial\tilde{\psi}_0^2}{\partial r}=\frac{\partial\tilde{\phi}_0^2}{\partial r} \tag{56}$$

with $\tilde{\psi}_0^2=0$ when $z=0,1$, and $\tilde{\psi}_0^2=0$ when $r=\delta$. Since it has been shown that $c_0^2=0$ and hence that $\hat{\psi}_0^2=0$, it follows that the matching condition for $\tilde{\psi}_0^2$ is the sum of the terms in the solutions for $\hat{\psi}_{2n}^2$ that jump to $O(\lambda^2)$ when matching with the hot end region. By noting the Rayleigh number dependence of $\tilde{\phi}_0^2$ and of the matching terms that jump order, we can write $\tilde{\psi}_0^2=\mathrm{Ra}\,(\tilde{\psi}_0^2)'$. The governing equation for $(\tilde{\psi}_0^2)'$ is given by Eq. (56) with $\tilde{\psi}_0^2$ replaced by $(\tilde{\psi}_0^2)'$, and $\tilde{\phi}_0^2$ replaced by $(\tilde{\phi}_0^2)'$. The matching condition is

$$(\tilde{\psi}_0^2)'\sim A^2(\hat{\psi}_2^2)'+A^4(\hat{\psi}_4^2)'+A^6(\hat{\psi}_6^2)'+\ldots \tag{57}$$

The solution of Eq. (56) subject to the appropriate boundary and matching conditions has been obtained numerically and the results for $\delta=0.1$,1 and 10 are plotted in Fig. 5 (see Table 1 for details of the contour values), where it is noted that the summation in Eq. (57) was truncated at $O(A^{10})$ to obtain the numerical solutions. It is seen that the $(\tilde{\psi}_0^2)'$ perturbation consists of four counterrotating cells with two of the cells confined near the inner cylinder and the other two cells extending into the intermediate matching region. For smaller values of δ, the cells near the inner cylinder are relatively narrower and the magnitude of the stream function perturbation is increased, again showing the increased influence of curvature at small δ.

The energy equation at $O(\lambda^3)$ in the hot end region is given by

$$\frac{\partial^2\tilde{\phi}_0^3}{\partial r^2}+\frac{1}{r}\frac{\partial\tilde{\phi}_0^3}{\partial r}+\frac{\partial^2\tilde{\phi}_0^3}{\partial z^2}=\frac{\mathrm{Ra}}{r}\left(\frac{\partial\tilde{\psi}_0^1}{\partial r}\frac{\partial\tilde{\phi}_0^2}{\partial z}-\frac{\partial\tilde{\psi}_0^1}{\partial z}\frac{\partial\tilde{\phi}_0^2}{\partial r}\right)-\frac{\mathrm{Ra}}{r^2}\frac{\partial\tilde{\psi}_0^2}{\partial z} \tag{58}$$

subject to $\tilde{\phi}_0^3=0$ when $r=\delta$, and $\dfrac{\partial\tilde{\phi}_0^3}{\partial z}=0$ when $z=0,1$. The matching condition for $\tilde{\phi}_0^3$

$$\tilde{\phi}_0^3\sim D_0^3+A^2\hat{\phi}_2^3+A^4\hat{\phi}_4^3+A^6\hat{\phi}_6^3+\ldots \tag{59}$$

where it is noted that previous matching has shown that $C_0^3=c_0^3=0$, so that the homogeneous solution $(\tilde{\phi}_0^3)_h$ vanishes. The $\hat{\phi}_{2n}^3$ terms represent core region solutions that jump order when matching with the hot end region. The matching condition and Eq. (58) are such that $\tilde{\phi}_0^3$ can be decomposed as $\tilde{\phi}_0^3=(\mathrm{Ra})^2\,(\hat{\phi}_0^3)'$ with the constant D_0^3 written as $D_0^3=(Ra)\,(D_0^3)'$.

Following Leppinen (2002), the unknown constant $(D_0^3)'$ is determined as part of the solutions to Eq. (58). In particular, matching condition (59) is replaced by

$$\frac{\partial(\tilde{\phi}_0^3)'}{\partial r}=\frac{\partial}{\partial r}\left(A^2(\hat{\phi}_2^3)'+A^4(\hat{\phi}_4^3)'+A^6(\hat{\phi}_6^3)'+\ldots\right) \tag{60}$$

and the value of $(D_0^3)'$ is determined from the numerical solutions of $(\tilde{\phi}_0^3)'$ by calculating

$$(\Delta_0^3)'=(\tilde{\phi}_0^3)'-(A^2(\hat{\phi}_2^3)'+A^4(\hat{\phi}_4^3)'+A^6(\hat{\phi}_6^3)'+\ldots) \tag{61}$$

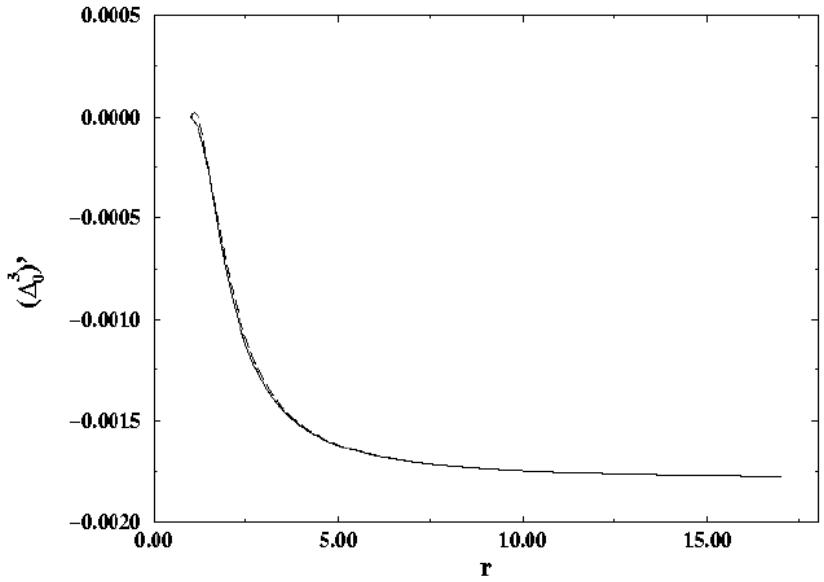

Figure 5. The $O(\lambda^2)$ stream function perturbation $(\tilde{\psi}_2^2)'$ in the hot end region when a) $\delta = 0.1$, b) $\delta = 1$, and c) $\delta = 10$. (See Table 1 for details.)

and then examining the value of $(\Delta_0^3)'$ throughout the intermediate matching region. In the numerical implementation, the summations in Eqs. (60) and (61) were truncated at $O(A^{10})$.

The numerical solution for $(\tilde{\phi}_0^3)'$ when $\delta = 1$ was used to generate the plot of $(\Delta_0^3)'$ in Fig. 6. The solid curve corresponds to the minimum value of $(\Delta_0^3)'$ over the interval $0 \le z \le 1$ as a function of r, while the dashed curve corresponds to the maximum value. Figure 6a plots $(\Delta_0^3)'$ versus r, while Fig. 6b replots the same data as $(\Delta_0^3)'$ versus $1/r^2$. The data in Fig. 6b can be extrapolated to show that $(D_0^3)'$ approaches a constant value of $(D_0^3)' = -1.81 \times 10^{-3}$ in the intermediate matching region. Thus, $D_0^3 = (\mathrm{Ra})^2 (D_0^3)'$ is the first nonzero value of D_0^k and this term forces the first convective contribution to the core region solutions at $O(\lambda^4)$ since $c_0^4 = D_0^3$.

In principle, it is possible at this point to continue to higher orders in λ to determine values of D_0^k for $k > 3$. To do so, however, would require the numerical solution of an ever-increasing number of equations. Since the effort required to solve these equations in the hot end region is in effect comparable to the effort that would be required to solve the full nonlinear equations in the entire annular enclosure, it has been decided to terminate the asymptotic analysis at $O(\lambda^3)$.

THE INFLUENCE OF VARYING δ

The results presented in Fig. 6 show that D_0^3 is nonzero for the specific value of $\delta = 1$. The results for δ varying between 0.1 and 10 are given in Fig. 7, which plots $(D_0^3)'$ as a function of δ. Figure 7 shows that $(D_0^3)'$ is a decreasing function of δ. For a fixed (but small) value of A, the asymptotic solutions for the case when δ is of $O(1)$ should approach the asymptotic solutions for the case when δ is of $O(1/A)$ when δ becomes sufficiently large. Since the first convective contribution in the core region occurs at $O(A^2)$ for the case when δ is of $O(1/A)$, it follows that the $O(\lambda^4)$ convective contribution in the core region for the case when δ is of $O(1)$ must vanish for large δ. This is indeed consistent with the results plotted in Fig. 7.

NUSSELT NUMBER

A fundamental quantity when examining natural convection within enclosures is the Nusselt number Nu, which represents the ratio of the total rate of heat transfer to some relevant conduction heat transfer scale. For convection in the annular gaps considered here, it is the radial heat transfer between the inner and outer cylinder that is of interest and Nu is defined as

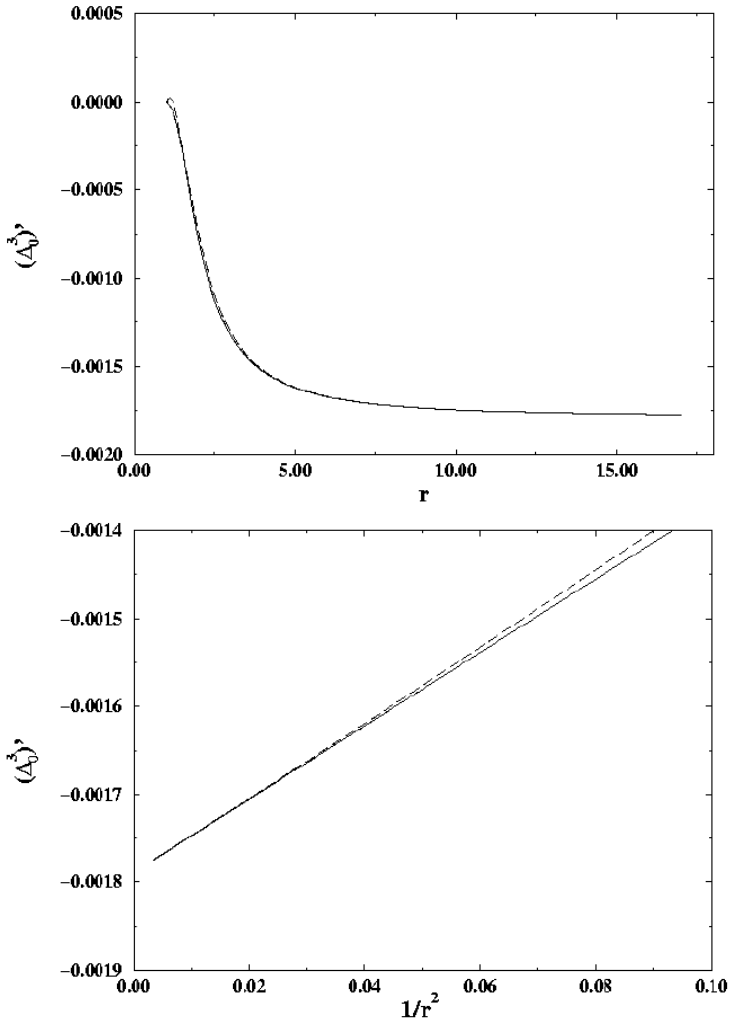

Figure 6. Maximum (dashed line) and minimum (solid line) of $(\Delta_0^3)'$ as a function of r when $\delta = 1$. In a) $(\Delta_0^3)'$ is plotted versus r while in b) $(\Delta_0^3)'$ is plotted versus $1/r^2$.

$$\mathrm{Nu} = \frac{q^*_{\mathrm{total}}}{2\pi h r_1 k\,(T_1 - T_2)/l} \tag{62}$$

where q^*_{total} is the integrated radial heat transfer through any concentric cylindrical shell between the inner and outer cylinder and k is the thermal conductivity of the fluid in the annular cavity. In terms of the nondimensional variables defined in Eq. (5), the Nusselt number is evaluated as

$$\mathrm{Nu} = \frac{r'}{\Gamma}\int_0^1 \left(\mathrm{Ra}\,Au\theta - \frac{\partial\theta}{\partial r}\right)_{r=r'} dz \tag{63}$$

where $\delta \le r' \le \delta + 1/A$. Note that global conservation of energy implies that Nu is independent of the choice of r' used in Eq. (63). Substituting the core region solutions into Eq. (63) gives

$$\mathrm{Nu} = -\frac{1}{\Gamma}\left(\lambda + c_0^4\lambda^4\right) + O(\lambda^5) \tag{64}$$

where it is noted that the asymptotic parameter λ is negative with

$$\lambda = \frac{1}{\ln\left(\dfrac{A\delta}{A\delta + 1}\right)}.$$

The quantity c_0^4 in Eq. (64) is a function of δ with $c_0^4 = (\mathrm{Ra})^2\,(D_0^3)'$.

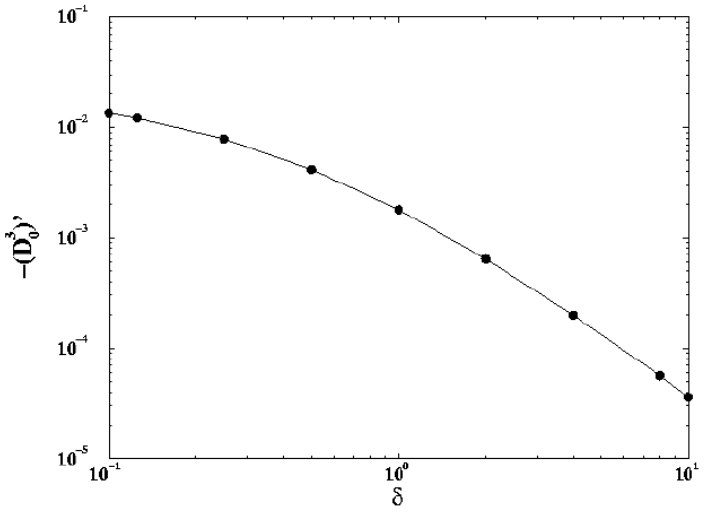

Figure 7. Variation of $(D_0^3)'$ with δ.

SUMMARY

This paper has presented asymptotic solutions for convection in shallow cylindrical annuli filled with a porous medium as the aspect ratio $A \to 0$. This paper extends the results of Pop et al. (1998) who considered convection in shallow cylindrical annuli with $\delta = O(1/A)$ where δ is the dimensionless radius of the inner cylinder. The current results are for the case of $\delta = O(1)$. In both cases, the analysis involves matching solutions in the end regions near the inner and outer cylinders with solutions in a central core region. When $A \to 0$ with δ of $O(1)$, the asymptotic analysis is considerably complicated by the fact that terms in the core region solutions jump order when matching with solutions in the hot end region. It has been shown that curvature effects dramatically dictate the order at which convection influences the core region solutions (i.e., there is a Ra number dependence). When δ is of $O(1/A)$, the first convective influence occurs at $O(A^2)$. When δ is of $O(1)$, the first convective influence occurs at $O(\lambda^4)$ where $\lambda = \dfrac{1}{\ln\left(\dfrac{A\delta}{A\delta+1}\right)}$, while small, is a much larger asymptotic parameter than A as $A \to 0$. Thus the asymptotic solutions as $A \to 0$ are fundamentally different when δ is of $O(1/A)$ and when δ is of $O(1)$. Pop et al. (1998) considered convection when $\delta = O(1/A)$ with both $\mathrm{Ra} = O(1)$ and $\mathrm{Ra} = O(1/A)$. This paper has only considered convection with $\delta = O(1)$ and $\mathrm{Ra} = O(1)$ as $A \to 0$. The case of convection with $\delta = O(1)$ and $\mathrm{Ra} = O(1/A)$ as $A \to 0$ has yet to be solved. To the best knowledge of the authors, there are no experimental results available with which to compare the results presented herein.

REFERENCES

Hinch, E. J., *Perturbation Methods*, Cambridge University Press, Cambridge, England, 1991.

Leppinen, D. M., Natural convection in shallow cylindrical annuli, *Int. J. Heat Mass Transf*er., vol. 45, pp. 2967–2981, 2002.

Lewis, S., Bassim, A. P., and Rees, D. A. S., The stability of vertical thermal boundary layer flow in a porous medium, *Eur. J. Mech. B: Fluids*, vol. 14, pp. 395–408, 1995.

Pop, I., Rees, D. A. S., and Storesletten, L., Free convection in a shallow annular cavity filled with a porous medium, *J. Porous Media*, vol. 1, pp. 227–241, 1998.

Prasad, V., and Kulacki, F. A., Natural convection in a vertical porous annulus, *Int. J. Heat Mass Transfer*., vol. 27, pp. 209–219, 1984.

Prasad, V. and Kulacki, F. A., Natural convection in porous media bounded by short concentric vertical cylinders, *Trans. ASME, J. Heat Transfer*., vol. 107, pp. 147–154, 1985.

Prasad, V., Kulacki, F. A., and Kulkarni, A. V., Free convection in a vertical, porous annulus with constant heat flux on the inner wall — Experimental results, *Int. J. Heat Mass Transfer*., vol. 29, pp. 713–723, 1986.

Rees, D. A. S., Nonlinear wave stability of vertical thermal boundary layer flow in a porous medium, *J. Appl. Math. Phys*. (Z.A.M.P.), vol. 44, pp. 306–313, 1993.